Gaussian Models for CSI Fingerprinting in Practical Indoor Environment Identification

Josyl Mariela Rocamora*[†], Ivan Wang-Hei Ho* and Man-Wai Mak*

*Department of Electronic and Information Engineering, The Hong Kong Polytechnic University

[†]Department of Electronics Engineering, University of Santo Tomas, Manila, Philippines

josyl.rocamora@connect.polyu.hk, {ivanwh.ho, enmwmak}@polyu.edu.hk

Abstract—It is not uncommon to experience highly dynamic channels in indoor environments due to time-varying signals as well as moving reflectors and scatterers. This greatly affects the performance of wireless sensing systems that use received signal strength indicator (RSSI) and channel state information (CSI) fingerprints for indoor positioning and event detection. Solutions to this dynamic channel problem often involve labor-intensive database maintenance and customized hardware. With this, we present Gaussian models that can withstand temporal and environmental dynamics in practical indoor environments using off-the-shelf devices in this paper. Although systems employing Gaussian models have been previously proposed in the literature, most systems use RSSI instead of CSI to represent the wireless channel. By using a Gaussian distribution to model CSI fingerprints, which offer more abundant information regarding the channel dynamics than RSSI, we can exploit the variance inherent in the wireless channels. Our experiments demonstrate that the Gaussian classifier incurs minimal delay of less than 4 seconds and achieves high classification accuracy compared to other techniques. In particular, it achieves up to 50% and 150% performance improvement over the time-reversal resonating strength (TRRS) and the support vector machines (SVM) methods, respectively.

Index Terms—Channel State Information (CSI), Gaussian Classifiers, Clustering, Wireless Sensing

I. INTRODUCTION

Wireless sensing applications include positioning, human behavior recognition, motion tracking, and event monitoring under indoor environments [1]. For instance, indoor positioning systems (IPS) can localize target devices at meter-level resolution and even up to centimeter-level with the help of spatial or frequency diversity [2]. Aside from positioning, sensing systems may also operate in other applications such as human presence detection [3], proximity detection [4], environment detection [5], tracking and trajectory prediction [6]. Human movements such as standing and sitting can also be distinguished using wireless signals [3]. Motion tracking using IPS can be achieved with the use of inertial measurement units (IMU) [7]. Detecting line-of-sight (LOS) or non-line-of-sight (NLOS) is another function of these systems [5].

These wireless sensing systems primarily operate using range-based or range-free techniques [1]. Range-based techniques refer to the use of estimated distances based on the measured signal strengths or angles from several access points (AP) to map the target's position in space geometrically. These techniques, also known as ranging, rely on LOS to accurately estimate the distance between the anchor point and the target.

On the other hand, range-free strategies employ fingerprinting methods, wherein a unique wireless signature represents each position or environment. Such a system classifies new data by finding the best match in a database of fingerprints using similarity functions, statistical techniques, and machine learning algorithms [2]. Unlike ranging, fingerprinting-based systems can operate well in both LOS and NLOS conditions and can be accomplished with a single AP only. Fingerprints are generated based on wireless measurements, such as received signal strength indicator (RSSI) or channel state information (CSI). Two types of CSI are channel impulse response (CIR) in the time domain and channel frequency response (CFR) in the frequency domain [8].

An advantage of CSI is its intrinsic ability to represent multipath effects, for which RSSI is not able to identify. Unlike RSSI, CSI is more commonly used for human sensing because it offers richer information about the channel [1]. Compared to RSSI-fingerprinting, CSI-based systems can achieve better performance (e.g., centimeter-level accuracy) and can be easily enhanced through spatial or frequency diversity. For instance, we can obtain more information from CFRs by concatenating several samples collected across different links or different frequency bands [9], and having more information can further improve the classification accuracy [10].

One challenge of fingerprinting-based systems is the sensitivity to temporal and environmental changes [2]. Since wireless signals vary over time due to human movement or changes in the indoor layout, past fingerprints may no longer be relevant. RSSI levels may change up to 10 dB in five minutes when the environment is highly dynamic [11]. CFR phase information can also vary in seconds, thereby necessitating sophisticated phase compensation methods during data collection [9]. If the channel has significantly changed, such dynamics would seriously affect the performance of fingerprinting-based methods [12].

Some solutions to the problem of environment dynamics include regularly updating the fingerprint database [12] and modeling theoretical fingerprints [13]. For instance, [12] suggested a technique called continuous fingerprint appending (CFA), where several samples from each point of interest were recorded to improve localization performance. This solution, however, requires regular site surveys and fingerprint preprocessing, which is labor-intensive. In contrast, another solution is to simulate CIR fingerprints of ultra-wideband (UWB)

signals, given the floor plan and the map of large obstacles [13]. However, if the obstacles in the room are moved, then the system requires recalibration.

In this paper, we explore Gaussian models as a solution to the dynamic channel problem in wireless sensing. Modeling the distribution of CSI data as a Gaussian density helps exploit the variance and dynamics inherent in the data. Several other wireless sensing applications also use Gaussian models, such as image patches for vision-based tracking [14] and static channel information for accurate CSI estimation [15].

Specifically, we apply Gaussian classifiers to combat against temporal and environmental variations in CSI-based indoor environment identification. We first discuss Gaussian-based wireless sensing systems in Section II. It is then followed by Gaussian model along with low-dimensional embedding and clustering performance criteria in Section III. We then compare the classification performance and delay of our Gaussian classifiers against previous algorithms in Section IV. In Section V, an extension of our work to a mixture model including its applications is briefly discussed. Finally, we summarize our findings in Section VI.

II. Indoor Positioning and Environment Identification using Gaussian Models

Table I lists indoor positioning and environment detection systems based on Gaussian models. These systems use Gaussian densities to model different types of data, e.g., RSSI radio maps, RSSI additive noise, and CFR per-subcarrier structures. The basic idea is that these data are position-dependent. For example, the RSSI histograms at different locations have different shapes [19]. The CFRs at a unique location have a statistical structure, that is, the complex subcarriers of the CFR form clusters, where each cluster follows a Gaussian distribution [4]. If there are few statistical structures, the CFR is stable, and the localization performance is good.

Because wireless channels can be modeled statistically, the aforementioned systems can perform positioning and detection. Ranging-based RSSI location estimation can be achieved by: (1) multilateration after modeling noise as a mixture of Gaussians [23] and (2) quadrilateral positioning after filtering out unwanted samples [22]. Based on maximum likelihood, a classifier can also be trained to output the posterior probability, which can be utilized for classifying RSSI fingerprints [16] [17] [18] [19] [21] or CFR fingerprints [4]. Alternatively, RSSI generated according to a Gaussian model can be utilized for training classifiers that can achieve similar performance as a system trained using actual RSSI data [20].

Most systems utilize RSSI from WiFi APs as a physical representation of the wireless channel, while other implementations use RSSI from GSM base stations [17], from Zigbee nodes [23] and from customized hardware tuned at 433 MHz [18]. Besides, most of these systems do not consider practical situations involving temporal stationarity and environmental dynamics; the time frame between training and testing data acquisition must be short, e.g., minutes or hours. WiFi positioning accuracy is over 70% for static scenarios, but less than 70% for dynamic cases (e.g., heavy indoor foot traffic) [16]. Only the PinLoc system in [4] utilizes CSI, specifically CFR, to represent unique spots in various places such as classrooms, museums, and cafes. One simple experiment showed that the accuracy was degraded from 89% to 70% when the test was conducted months after the original site survey.

With this, we utilize Gaussian distribution to model our CSI data, specifically CFR data, with temporal and environmental variabilities. Unlike PinLoc [4], our system does not require a high sampling rate of one packet per second nor utilize compensation techniques to stabilize the CFR phases. The subcarrier phase is often erratic and is dependent on hardware stability; it also requires excellent timing and synchronization [10]. Our system, on the contrary, embraces the variability introduced by this phase information to generate clusters and only acquires CFR fingerprint once every few minutes or every hour. Finally, our system can do classification based on a single test data, this is in contrast to PinLoc that determines an estimate after receiving a series of packets.

III. Implementation of Practical Indoor Environment Identification

A. System Overview

Figure 1 shows our Gaussian-based indoor environment identification system, which involves two phases, namely, offline (training) and online (testing). In the offline phase, CSI fingerprints are preprocessed then utilized for training the Gaussian models. In the online phase, we apply preprocessing on a CSI testing fingerprint using the stored training parameters. We then predict the class of the preprocessed testing data by using the Bayes' classification rule.
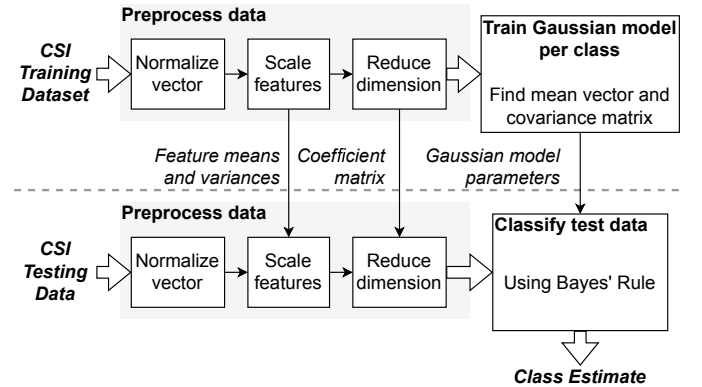

Fig. 1: Indoor Environment Identification System

B. CSI Dataset and Experimental Setup

We consider two practical indoor environments in the Hong Kong Polytechnic University, which we referred to as rooms A and B in this paper. Two sets of USRP N210 software-defined radio (SDR) and a computer were utilized for data collection, as shown in Fig. 2; one set operated as the transmitter, and the other acted as the receiver similar to our previous works [2] [8] [10]. Transmitter-Receiver (TX-RX) separation in the rooms was approximately three meters.

TABLE I: Recent indoor positioning and environment detection systems based on Gaussian models

| Ref.	Gaussian model application	Technique	Preprocessing	Dynamic tests?	Classification results (accuracy, error, speed)
[4]	CFR per-subcarrier model	Min. Mahalanobis distance	Data sanitization	Yes	89% accuracy, 6% false positive probability
[16]	RSSI radio map	Bayes' rule	None	Yes	$<70\%$ accuracy (dynamic case)
[17]	RSSI radio map	Bayes' rule	PCA	No	78.8% accuracy
[18]	RSSI radio map	Bayes' rule	Feature scaling	No	70–72% accuracy (if HMM filter)
[19]	RSSI radio map	Iterative elimination	Feature scaling	No	85% accuracy, 1-sec speed
[20]	RSSI radio map	kNN, SVM, etc.	None	No	70–80% accuracy
[21]	RSSI radio map	Particle filter	None	No	$p(|e| <= 10m) = 0.95$, 1-sec speed
[22]	RSSI sample filter	Quadrilateral positioning	None	No	$\mathbb{E}[|e|] = 0.48m$
[23]	RSSI additive noise	Ranging	None	No	$p(|e| <= 2m) = 0.63$

(a) Room A   (b) Room B
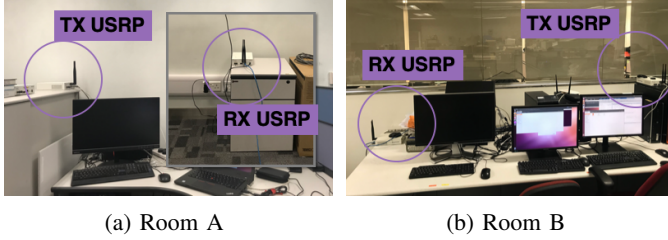
Fig. 2: Practical indoor environments

Following a similar framework as IEEE 802.11a, the SDRs were set to transmit OFDM symbols at 10-MHz channels with 52 data subcarriers out of 64 usable subcarriers. We utilized 10 channels from 3.16 to 3.25 GHz to avoid interference from indoor wireless devices. Thus, each fingerprint contains a total of 520 subcarriers ($10 \; \texttt{channels} \times 52 \frac{\texttt{subcarriers}}{\texttt{channel}}$) and is saved as a complex vector of 520 dimensions.

Figure 3 shows CSI fingerprints, where magnitude represents power, while phase represents the delay. CSI can easily capture human activities and environmental changes [9], as well as the effects of time on the channel [27]. As shown in the figure, CSI fingerprints collected at daytime and nighttime can be visually distinguished, as well as those from different environments. Furthermore, we can see that the phase information significantly changed with time.

A site survey for a total of 680 collection periods was conducted at different timeslots for four weeks. Normal office operations continued during data collection, and people were not restricted from moving in and out of the rooms. Objects such as doors, tables, chairs, and other obstructions could be moved. Since 10 fingerprints per period were recorded, the total number of fingerprints is 6800, where 50% is from Room

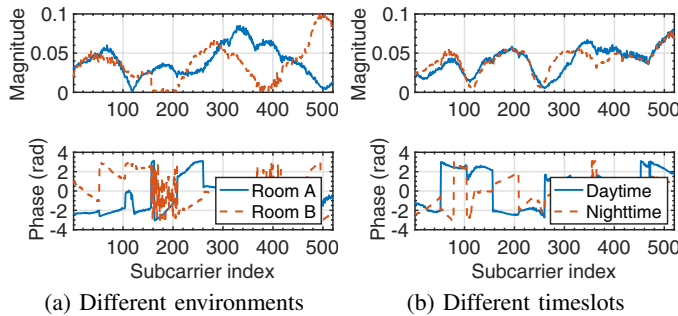(a) Different environments   (b) Different timeslots

Fig. 3: CSI Fingerprints with 100-MHz bandwidth

A and the other 50% is from Room B. The training and testing datasets consist of 5300 fingerprints collected over several days in Sept. 2019 and 1500 fingerprints acquired during the 1st week of Oct. 2019, respectively.

Since most machine learning techniques operate on real-valued vectors and matrices, we transform our complex-valued data to real-valued data. Unlike other works [4] [8] [10], our system does not require intricate phase sanitization methods, but exploits the inherent variance in the phase information to generate a universal model. Hence, we convert each 520-dim complex fingerprint to either:

1) 520-dim magnitude-only fingerprint where only subcarrier magnitudes are retained.
2) 1040-dim magnitude-phase fingerprint where both subcarrier magnitudes and phases are concatenated.

C. Data Preprocessing

As shown in Fig. 1, data preprocessing involves three parts. Each fingerprint is converted to a unit vector so that the vector magnitude is equal to one. Only the shape of the fingerprint waveform is considered since signal amplitudes may vary depending on antenna gain and attenuation. We also applied scaling to enable equal weights among features since our features have different ranges of values. In Fig. 3, subcarrier magnitudes are less than 0.1 while subcarrier phases vary from $-\pi$ to π. Particulary, we applied standardization, wherein features have zero-mean and unit-variance.

Dimension reduction, also known as low-dimensional embedding, can be used to avoid the curse of dimensionality [24]. We applied low-dimensional embedding to reduce processing and remove correlated features, as well as visualize data. Redundant features may cause the covariance matrix to be singular and therefore non-invertible. Singular covariance matrix means the Gaussian density shrunk on a single data point and results in overfitting [25]. One way to measure non-singularity is to compute for the condition number of the covariance matrix, which should ideally be equal to 1.

Several low-dimensional embedding techniques are available such as Principal Component Analysis (PCA) and Linear Discriminant Analysis (LDA) [24]. PCA is an unsupervised algorithm that finds the directions that maximize variance; while LDA is a supervised technique that finds the separation among cluster means to minimize inter-cluster overlaps. Since data labels are unknown in real-time operation, LDA is not appropriate for our positioning system.

(a) Magnitude-only fingerprints
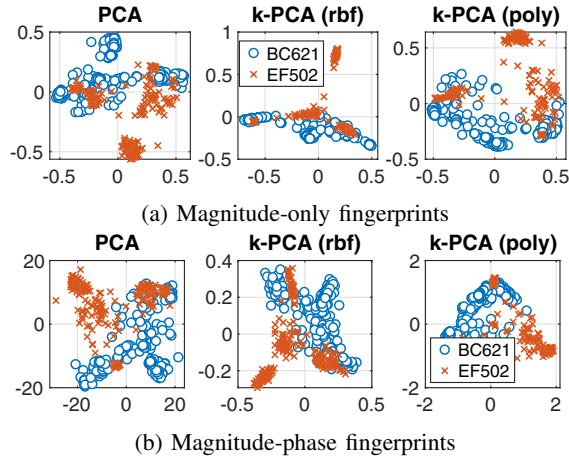

(b) Magnitude-phase fingerprints

Fig. 4: 2D plots of low-dimensional embedding techniques

Kernel techniques like k-PCA can be utilized in some cases when the dataset cannot be separated linearly [25]. These nonlinear dimension reduction techniques use kernel functions such as Gaussian radial basis function (rbf) and polynomial function (poly) to transform data into another subspace. The Gaussian and polynomial kernel functions are $k(\mathbf{x}, \mathbf{x}') = \exp(-\|\mathbf{x} - \mathbf{x}'\|^2 / 2\sigma^2)$ and $k(\mathbf{x}, \mathbf{x}') = (\mathbf{x}^{\mathrm{T}}\mathbf{x}' + c)^k$, respectively [25], where $\mathbf{x}$ and $\mathbf{x}'$ are input vectors. Kernel techniques are more computationally expensive because parameters (e.g., σ, k, c) must be properly tuned.

Figure 4 shows the training dataset reduced using different low-dimensional embedding techniques, where the x-axis and y-axis are the first two components of the reduced subspace. The figure shows the plots for both magnitude-only and magnitude-phase fingerprints. Variance retained after dimension reduction is at least 95% of the original variance for most scenarios. But for the k-PCA (rbf) of magnitude-phase data, only 70% of variance is retained to ensure that the resulting number of dimensions is in the same order as the original dimension count, and to avoid singular matrix. The condition number of the covariance matrix is 9.1e4 for magnitude-only fingerprints and 1.4e5 for magnitude-phase fingerprints before dimension reduction. After reducing the number of dimensions, the condition number is improved to 1.4e2 and 3.2e2 on average for magnitude-only and magnitude-phase fingerprints, respectively.

We apply PCA, k-PCA (rbf) and k-PCA (poly) using built-in Matlab functions and the Statistical Learning Toolbox from [26]. After parameter tuning simulation, we set the values of σ, k and c as listed in Table II. In the next subsection, we explore other criteria aside from visual 2D representation to evaluate the clustering performance.

TABLE II: Tuned parameters for k-PCA

Kernel function	for magnitude-only	for magnitude-phase
Gaussian rbf	$\sigma = 0.25$	$\sigma = 20$
Polynomial	$k = 1/2, c = 0$	$k = 1/3, c = 0$

D. Data Clustering Performance Evaluation

Clustering can be evaluated based on external or internal validation [24]. External validation requires additional information, such as labels. Internal validation focuses on the quality of cluster structures (e.g., compactness, separation). Examples of internal validation are the Silhouette coefficient (SC), Calinski-Harabasz (CH) index, and Davies-Bouldin (DB) index [24]. SC has values from -1 to +1 (ideal), where a value near +1 indicates highly dense clustering. CH index specifies the ratio of the inter-cluster variance to the intra-cluster variance. A good CH index is numerically large. DB index computes the similarities of one cluster to other clusters. Ideally, the DB index must be zero.

Tables III and IV show the clustering performance of the training datasets consisting of magnitude-only and magnitude-phase fingerprints, respectively. The number of dimensions after dimension reduction is listed for each technique. Since SC values are greater than zero, most techniques have decent clustering performance but some may be prone to overlapping clusters as the coefficient is near zero. Magnitude-only dataset without dimension reduction has the best clustering characteristics, according to the CH Index. On the other hand, both PCA and k-PCA (rbf) for magnitude-only fingerprints have small DB index values close to zero.

TABLE III: Clustering magnitude-only fingerprints

Technique	# of dim	SC (nearest to 1)	CH Index (highest)	DB Index (nearest to 0)
None	520	0.456	2.42e3	1.47
PCA	8	0.175	1.62e3	0.93
k-PCA (rbf)	139	0.037	1.13e1	0.91
k-PCA (poly)	7	0.305	1.61e3	1.46

TABLE IV: Clustering magnitude-phase fingerprints

Technique	# of dim	SC (nearest to 1)	CH Index (highest)	DB Index (nearest to 0)
None	1040	0.186	6.65e2	2.28
PCA	214	0.132	7.15e2	1.80
k-PCA (rbf)	1117	0.005	1.96e1	2.21
k-PCA (poly)	21	0.228	9.83e2	2.02

E. Proposed Gaussian Models on Clustered Data

The multivariate Gaussian distribution is shown in (1) [25], where $\mathbf{x}$ is the data vector of size $n \times 1$. The parameters $\boldsymbol{\mu}$ and $\boldsymbol{\Sigma}$ are the mean vector of size $n \times 1$ and covariance matrix of size $n \times n$ of the Gaussian distribution, respectively. These values are calculated based on $\mathbf{X}$, which is an $m \times n$ data matrix, where m is the number of data samples. Since our dataset contains two classes (i.e., room A, room B), we train two multivariate Gaussian models, one for each class.

$$p(\mathbf{x}) = \mathcal{N}(\mathbf{x}|\boldsymbol{\mu}, \boldsymbol{\Sigma}) = \frac{\exp\left(\frac{1}{2}(\mathbf{x} - \boldsymbol{\mu})^{\mathrm{T}}\boldsymbol{\Sigma}^{-1}(\mathbf{x} - \boldsymbol{\mu})\right)}{\sqrt{(2\pi)^n|\boldsymbol{\Sigma}|}} \quad (1)$$

A Gaussian distribution with a full covariance matrix considers both the feature variances and covariances between different features. If the contours of such a Gaussian are

plotted in 2D, the model would have various shapes. Howe inverting the full covariance matrix Σ at high n may computationally expensive as there are $\frac{n(n+3)}{2}$ free paramet [25]. This problem can be mitigated by considering only diagonal elements of the covariance matrix so that the number of free parameters can be reduced to $2n$. A Gaussian dis bution using diagonal covariance matrix would only consi the feature variances. If the contours of such a Gaussian plotted in 2D, the model would show axis-aligned ellipses

We explore Gaussian densities using both full and diagonal covariance matrices. Without low-dimensional embedding, training Gaussian models with full covariance matrix using 5300 fingerprints takes around a minute of processing. On the other hand, the processing time is less than a second when the number of dimensions is reduced. We can classify new data $\mathbf{x}_n$ by determining which Gaussian distribution has most probably generated the data according to the Bayes' rule. Since the sample size for each class is equal, we can simply select the Gaussian model that returns the higher likelihood. For faster computation, we can calculate the log-likelihood function instead of the likelihood [25].

Table V shows the classification accuracy of each model based on classifying the training fingerprints. We look at the classification accuracy of the training fingerprints to validate how well our Gaussian classifier fits the training dataset. Based on the results, lower accuracy is usually evident for models with diagonal Σ, since some information is lost in converting the covariance matrix to a diagonal one. The processing time for Gaussian classifiers with diagonal Σ takes around 1–4 seconds, while those with full Σ requires up to a minute.

TABLE V: Classification accuracy based on training data

Technique	Magnitude-only		Magnitude-phase	
	full	diagonal	full	diagonal
None	0.9955	0.9038	0.9951	0.9042
PCA	0.9945	0.9802	0.9679	0.8177
k-PCA (rbf)	1.0000	0.8811	1.0000	0.7466
k-PCA (poly)	0.9943	0.9811	0.9977	0.9179

In summary, several Gaussian models shows good performance on the training dataset. In the next section, we compare these Gaussian classifiers to other previous algorithms such as TRRS w/ CFA and SVM, which were studied in [10]. TRRS is regarded as a similarity measure between two fingerprints [27], while SVM is a commonly-used classifier that identify the optimal hyperplane that separates two classes [2].

IV. CLASSIFICATION PERFORMANCE

Figure 5 shows the accuracy of various algorithms in classifying 1500 testing fingerprints. In most cases, our Gaussian classifiers can detect practical indoor environments with near-perfect accuracy. The Gaussian classifier with full covariance matrix performs 4–49% better than TRRS w/ CFA and 12–150% better than linear SVM. On the other hand, Gaussian classifier with diagonal covariance matrix has a performance improvement of 3–50% over TRRS, excluding the k-PCA (rbf) case, and 3–136% over SVM. Compared to TRRS and

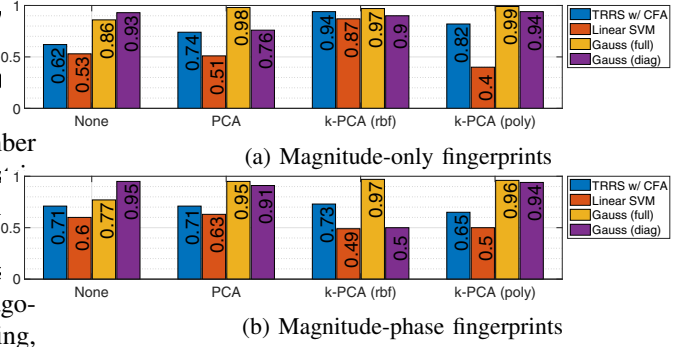(a) Magnitude-only fingerprints

(b) Magnitude-phase fingerprints

Fig. 5: Classification accuracy (0 to 1) based on testing data

SVM, the Gaussian classifiers have generally more consistent performance with and without phase information.

When the magnitude-phase fingerprints are reduced using k-PCA (rbf) and the off-diagonal elements of the covariance matrix are removed, the accuracy is poor since a significant amount of information is lost as the retained variance is 70% according to our results in Subsection III-C. Linear SVM for the k-PCA case shows a low accuracy of below 50%, which is no better than a random classifier. This particular case is primarily caused by the misclassification of all Room B testing data as well as few Room A testing data. Since the datasets are reduced by k-PCA, a non-linear dimension reduction technique, using also non-linear kernel for this SVM classifier (e.g., Gaussian kernel) may improve the accuracy from below 50% to around 60%.

In terms of processing time, our Gaussian classifiers with diagonal covariance matrices can typically classify 1500 testing fingerprints in 1–4 seconds, which is similar to other systems [19] [21] and as fast as our linear SVM. However, for full covariance matrices, the processing time may take seconds longer, depending on the number of dimensions n. On the other hand, classification using TRRS w/ CFA often takes the longest time (around 3–86 seconds), slowest for models without dimension reduction. Since TRRS w/ CFA has to calculate the pairwise correlation between training and testing fingerprints, the processing of a considerable number of high-dimensional data translates to longer computation time.

V. EXTENSION TO GAUSSIAN MIXTURE MODELS

One potential extension of our system is the use of Gaussian mixture models (GMM), which is the linear superposition of two or more Gaussian components [25]. GMMs can represent data from more complicated scenarios with several clusters. For instance, we can generate a 10-mixture GMM based on a PCA-reduced training dataset as shown in Fig. 6a. The dataset includes all 6800 fingerprints from Subsection III-B as well as additional 2190 fingerprints acquired at other rooms. We can let this GMM represent the fingerprints from one building as one class, then model other buildings and construct a multi-building classifier. Other than classification, we can also utilize GMM as a universal background model (UBM) in generating i-vectors, which can be used to improve class-specific deep neural networks and therefore minimize the cost

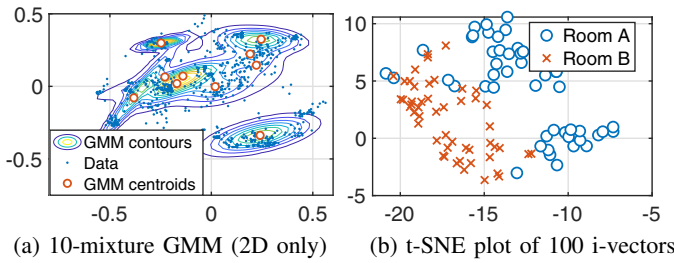(a) 10-mixture GMM (2D only)   (b) t-SNE plot of 100 i-vectors

Fig. 6: Sample GMM and its application to i-vectors

of label annotations [28]. Figure 6b shows a sample t-SNE plot of i-vectors generated from the 10-mixture GMM.

VI. CONCLUSION AND FUTURE WORK

In this paper, we have modeled Gaussian distributions of CSI data for indoor environment identification in practical scenarios. Various implementations have been evaluated using performance criteria such as Silhouette Coefficient, Calinski-Harabasz (CH) index, and Davies-Bouldin (DB) index.

Despite temporal and environmental changes, our Gaussian-based system can classify testing data collected 2–8 days after the site survey within 4 seconds with 95% accuracy. The system performs better than other previous algorithms, namely TRRS w/ CFA and Linear SVM, without the need of sophisticated phase compensation procedures. Finally, using low-dimensional embedding, we have enhanced the classification accuracy up to 99% and reduced the database storage space as fingerprints are transformed from 520-dim to 7-dim vectors while retaining 95% of the original variance.

We are working towards utilizing Gaussian mixture models (GMM) for more complicated experiments that cannot be modeled by a single Gaussian. Large-scale experiments, e.g., via introducing more number of environments, recording finer-grained resolution of positions, and considering longer time frame, would typically entail massive amounts of data. Such a GMM can be used for preparing a deep neural network (DNN) based on i-vectors to classify environments or positions without the need of extensive training database. This can significantly alleviate the problem of tedious site surveying in fingerprinting-based systems in the future.

REFERENCES

[1] Y. Ma, G. Zhou, and S. Wang, "WiFi sensing with channel state information: A survey," *ACM Comput. Surv.*, vol. 52, no. 3, pp. 46:1-46:36, Jun. 2019.

[2] J. M. Rocamora, I. W. Ho, M. Mak and A. P. Lau, "Survey of CSI fingerprinting-based indoor positioning and mobility tracking systems," *IET Signal Processing*, May 2020.

[3] Y. Gu, J. Zhan, Y. Ji, et al., "MoSense: An RF-based motion detection system via off-the-shelf WiFi devices," *IEEE IoT Journ.*, vol. 4, no. 6, pp. 2326-2341, Dec. 2017.

[4] S. Sen, B. Radunovic, R. R. Choudhury and T. Minka, "You are facing the Mona Lisa: Spot localization using PHY layer information," *Proc. ACM Int. Conf. MobiSys*, Lake District, UK, Jun. 2012, pp. 183–196.

[5] J. Liu, L. Wang, L. Guo, et al., "A research on CSI-based human motion detection in complex scenarios," *Proc. IEEE Int. Conf. Healthcom*, pp. 1-6, Oct. 2017.

[6] S. Shi, S. Sigg, L. Chen, and Y. Ji, "Accurate location tracking from CSI-based passive device-free probabilistic fingerprinting," *IEEE Trans. on Vehicular Technology*, vol. 67, no. 6, pp. 5217-5230, Jun. 2018.

[7] F. Zhang, C. Chen, B. Wang, et al., "WiBall: A time-reversal focusing ball method for decimeter-accuracy indoor tracking," *IEEE IoT Journ.*, vol. 5, no. 5, pp. 4031-4041, Oct. 2018.

[8] J. M. Rocamora, I. W. Ho and M. Mak, "The application of machine learning techniques on channel frequency response based indoor positioning in dynamic environments," *Proc. IEEE Int. Conf. SECON (Workshops)*, Hong Kong, pp. 1–4, Jun. 2018.

[9] C. Chen, Y. Chen, Y. Han, et al., "Achieving centimeter-accuracy indoor localization on WiFi platforms: A multiantenna approach," *IEEE IoT Journ.*, vol. 4, no. 1, pp. 122-134, Feb. 2017.

[10] J. M. Rocamora, I. W. Ho and M. Mak, "Fingerprint quality classification for CSI-based indoor positioning systems," *Proc. ACM MobiHoc (PERSIST-IoT Workshop)*, Catania, Italy, pp. 31-36, Jul. 2019.

[11] M. Youssef and A. Agrawala, "The Horus WLAN location determination system," *Proc. ACM Int. Conf. MobiSys*, WA, pp. 205–218, Jun. 2005.

[12] E. R. Magsino, I. W. Ho and Z. Situ, "The effects of dynamic environment on channel frequency response-based indoor positioning," *Proc. IEEE Int. Symp. PIMRC*, Montreal, QC, pp. 1–6, Oct. 2017.

[13] B. Großwindhager, M. Rath, J. Kulmer, et al., "SALMA: UWB-based single-anchor localization system using multipath assistance," *Proc. ACM Conf. SenSys, Shenzhen*, China, pp. 132-144, Nov. 2018.

[14] V. Anand, D. Pushp, R. Raj and K. Das, "Gaussian Mixture Model (GMM) Based Dynamic Object Detection and Tracking," *Proc. ICUAS*, Atlanta, GA, pp. 1365–1371, 2019.

[15] L. Haihan, Y. Li, S. Zhou and W. Jing, "A novel method to obtain CSI based on Gaussian Mixture Model and Expectation Maximization," *Proc. Int. Conf. WCSP*, Yangzhou, pp. 1–5, 2016.

[16] A. Haeberlen, E. Flannery, A. M. Ladd, et al., "Practical robust localization over large-scale 802.11 wireless networks," *Proc. ACM MobiCom*, PA, USA, pp. 70–84, 2004.

[17] B. Denby, Y. Oussar, I. Ahriz, and G. Dreyfus, "High-performance indoor localization with full-band GSM fingerprints," *Proc. IEEE ICC Workshops*, Dresden, Germany, pp. 1-5, 2009.

[18] K. Lee and L. Lampe, "Indoor cell-level localization based on RSSI classification," *Proc. CCECE*, Canada, pp. 21–26, 2011.

[19] M. Raitoharju, Á .F. García-Fernández, R. Hostettler, R. Piché, S. Särkkä, "Gaussian mixture models for signal mapping and positioning," *Signal Processing*, vol. 168, 2020.

[20] Ó. Belmonte-Fernández, R. Montoliu, J. Torres-Sospedra, et al., "A radiosity-based method to avoid calibration for indoor positioning systems," *Expert Sys. with App.*, vol. 105, pp. 89–101, Sep. 2018

[21] K. Kaji and N. Kawaguchi, "Design and Implementation of WiFi Indoor Localization based on Gaussian Mixture Model and Particle Filter," *Proc. Int. Conf. IPIN*, Sydney, NSW, pp. 1–9, 2012.

[22] C. H. Tseng and J. S. Yen, "Enhanced Gaussian mixture model of RSSI purification for indoor positioning," *Journ. of Systems Architecture*, vol. 81, pp. 1–6, 2017.

[23] Y. Zhang, S. Xing, Y. Zhu, F. Yan and L. Shen, "RSS-Based Localization in WSNs Using Gaussian Mixture Model via Semidefinite Relaxation," *IEEE Communications Letters*, vol. 21, no. 6, pp. 1329–1332, Jun. 2017.

[24] C. C. Aggarwal and C. K. Reddy, *Data clustering: Algorithms and applications*, 1st ed. CRC Press, 2014.

[25] C. M. Bishop, *Pattern recognition and machine learning*, Springer, 2006.

[26] D. Lin, "SL toolbox," www.mathworks.com/matlabcentral/fileexchange/12333-statistical-learning-toolbox, Sep. 2006, Accessed Feb. 1, 2020.

[27] C. Chen, Y. Chen, Y. Han, H. Lai, and K. J. R. Liu, "Achieving centimeter-accuracy indoor localization on WiFi platforms: A frequency hopping approach," *IEEE IoT Journ.*, vol. 4, no. 1, pp. 111-121, 2017.

[28] S. S. Xu, M. Mak and C. Cheung, "I-Vector-Based Patient Adaptation of Deep Neural Networks for Automatic Heartbeat Classification," *IEEE Journ. BHI*, vol. 24, no. 3, pp. 717–727, Mar. 2020.